

QUANTIFICATION OF INCORPORATION OF CELLULOSE NANOCRYSTALS AND CARBON NANOTUBES IN MELT COMPOUNDED THERMOPLASTICS USING RAMAN IMAGING

Anna E. Lewandowska¹ and Stephen J. Eichhorn¹

¹University of Exeter, College of Engineering, Mathematics and Physical Sciences, Stocker Road, Exeter, EX4 4QL, United Kingdom

Email: A.E.Lewandowska@exeter.ac.uk, Web Page: <http://www.exeter.ac.uk/>

Keywords: Raman Imaging, Chemical Imaging, Cellulose Nanocrystals, Multiwalled Carbon Nanotubes, Thermoplastics

Abstract

This contribution will present the advantages of using Raman imaging as a complementary method to conventional techniques for investigating composite morphology. Two series of polyethylene based composites were prepared by melt compounding using cellulose nanocrystals (CNCs) and multiwalled carbon nanotubes (MWCNTs) as nano fillers. The cross sectional areas of nano composite filaments extruded from the compounder were investigated using confocal Raman microscopy. A protocol based on the combination of the structural and chemical “fingerprint” of a spectroscopic analysis with optical microscopy was developed. Raman images reveal the distribution of the fillers in the polyethylene matrix, while chemical images showed the degree of mixing between the fillers and matrix. The CNCs exhibited a lower degree of distribution than MWCNTs in polyethylene. The hydrophilic nature of CNCs induced the formation of hydrogen bonding between the nanoparticles increasing their tendency to agglomerate in nonpolar matrices. However a certain degree of mixing between CNCs and HDPE has been observed by Raman imaging.

1. Introduction

The production of nano composites with enhanced mechanical properties requires good mixing and/or dispersion of fillers in the matrix and strong interfacial adhesion between both phases. Increasing attention is being focused on thermoplastics matrices, since they are potentially re-moldable, low cost and can be formed using mature technology (extrusion, injection molding etc.). These traditional processing routes are also relevant for the incorporation of reinforcing nanofillers, including cellulose nanocrystals and carbon nanotubes. Nanocomposites such as these are often studied using scanning electron microscopy (SEM) [1, 2], differential scanning calorimetry (DSC) [1, 2], thermogravimetric analysis (TGA) [1], dynamic mechanical analysis (DMA) [3], and mechanical tests [1, 3]. These techniques give an answer related to their physicochemical properties without the quantitative evaluation of the quality of mixing between fillers and matrices.

Raman spectroscopy has been widely used for *in situ* characterisation of the solid materials [4] and in the characterisation of the surface of materials under working conditions [5]. Progress in spectroscopic imaging has opened up new capabilities for this technique providing exceptional advantages in delivering detailed structural and molecular information on composite morphology. The combination of Raman spectroscopy with confocal microscopy allows the rejection of out-of-focus Raman scattering generating images with less background and improved resolution. Raman imaging has been used to study cellulose nanocrystals-polypropylene composites [6], biomaterial degradation *in vivo* [7], the characterization of multilayer films [8] and compatibility of polymer blends [9].

This work focuses on the use of Raman imaging combined with chemical imaging and image analysis to evaluate the quality of CNCs-HDPE and MWCNTs-HDPE composites. Additionally, the quantitative assessment of the mixed and pure composite components gives an answer on the qualitative-quantitative properties of composites.

2. Experimental

Freeze-dried cellulose nanocrystals were purchased from the University of Maine, Process Development Centre; USA. Multiwalled carbon nanotube fillers were used as a master batch of 25% in weight of MWCNT dispersed in high-density polyethylene (Graphistrength C HDPE1-25) purchased from Arkema. High density polyethylene (Arboblend HDPE) was supplied by Tecnar GmbH, while maleic anhydride grafted polyethylene (A-C 575A, MAPE copolymer) was provided by Honeywell. All HDPE composites were prepared by melt-compounding in a counter rotating twin-screw extruder (HAAKE Rheomex CTW5, Thermo Fisher Scientific) which formed filaments with a diameter ~2 mm. Composites containing CNCs as fillers were extruded at a temperature of 160 °C. The mixing speed was 70 rpm for 7 min. Prior to extrusion, the fillers and compatibilizer were blended in a mortar for 2 minutes. Subsequently, the powder/HDPE matrix was added and the components were mixed in a mortar for a further 8 minutes. The mixture was dried in a vacuum oven at a temperature of 60°C for 24h to remove humidity. Composites containing MWCNTs as fillers were extruded at a temperature of 210 °C. The mixing speed was 50 rpm for 10 min. Prior to extrusion the pellets of the master batch of MWCNTs and HDPE were mixed.

The morphology of the cross-section of the composite filaments was studied using a HITACHI S3200N SEM-EDS scanning electron microscope (SEM) operated at an acceleration voltage of 10 kV. The slices of filament were fixed on metal stubs using carbon tape and sputter-coated at ~20 mA with a ~10 nm layer of gold. The magnifications used for the collection of SEM images were 3000×. Raman spectroscopy was performed using a confocal Raman microscope, Alpha300 (WITec) equipped with a thermoelectrically cooled CCD detector (down to - 61 °C). A 532 nm wavelength laser was used to collect Raman spectra from cross-sections of composite filaments. During the mapping of the CNCs-HDPE composites the power of the laser was ~13 mW. It was reduced to ~2.3 mW for MWCNTs-HDPE composites to minimize heating of the samples. A 50× objective lens was used for backscattered light collection. The spectrometer grating was 600 g/mm, BLZ = 500 nm. Raman images were recorded in an area of 50×50 μm² with a step size of 0.2 μm and an exposure time of 0.1 s and one accumulation. A total of 62500 Raman spectra were measured for each map. The average number of maps per composite was five. WITec Project Plus software was used to analyze Raman images and to convert them into chemical images. These chemical images were subsequently analyzed using Image-J software to estimate the area in μm² and the percentage of the area related to each component of the chemical image. The extraction of the objects was performed using an automated threshold with the algorithm IsoData.

3. Results and Discussion

Figure 1 illustrates the representative SEM images of cross-sectional areas of HDPE composites containing 1.25% of CNCs (Fig. 1A) and 1.25% of MWCNTs (Fig. 1B). The surface of the cross-sectional areas of composites containing CNCs is smooth with noticeable aggregates of cellulose. The aggregates of freeze-dried CNCs form irregular shapes within the volume of polyethylene (Fig. 1A). SEM images reveal also the presence of voids between HDPE matrices and CNC aggregates. Their presence is as a result of two physical properties. The first is a poor interfacial adhesion between the CNCs and HDPE.[10] The second is the process of the cryo-microtome cutting at a temperature of - 22°C, since the orientation of the main axis of the voids is consistent with the direction of cutting. The process of cutting could potentially induce a drawing out of the aggregates from the matrix, since polyethylene maintains some plasticity at this temperature. The surface of cross-sectional area of

MWCNTs-HDPE composites is smooth without voids (Fig. 1B). The scratches visible on the surface originate probably from the blade of the knife used for cryo-microtome cutting. It seems that these samples are free of aggregates during the melt compounding process with HDPE. Although SEM images confirm the existence of aggregates (or not) of nanofillers in HDPE, a question still remains over the degree of mixing of fillers in the thermoplastic polymer.

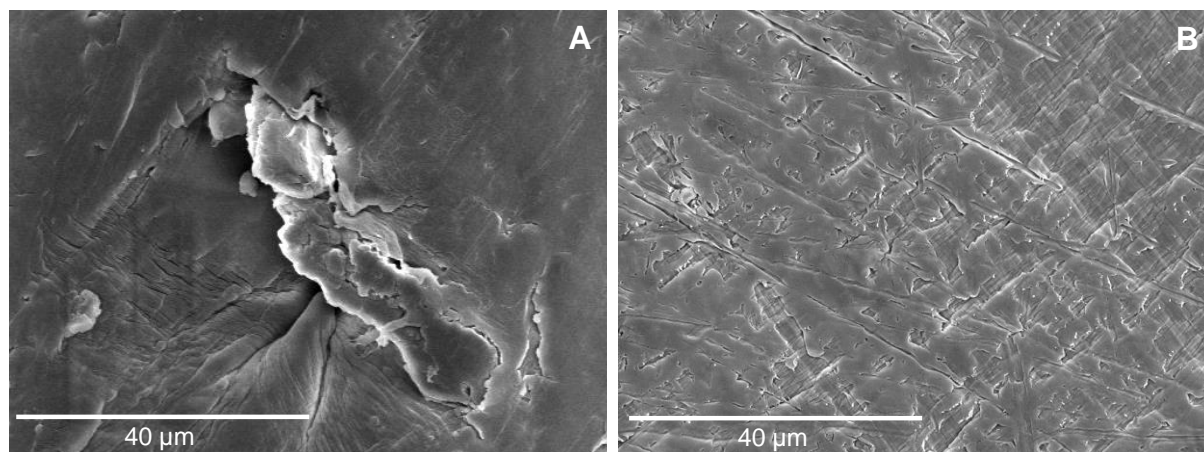


Figure 1. SEM images of cross-section area of cryo-microtome composites at a magnification 3000×: (A) 1.25% CNCs-HDPE, (B) 1.25% MWCNTs-HDPE.

Raman imaging combines a structural and chemical “fingerprint” of spectroscopic analysis with a visualization using optical microscopy. This combination facilitates a description of the quality of composite interfaces, and an estimation of the degree of mixing between the fillers and the thermoplastics. For these purposes characteristic Raman bands are used for distinguishing each of the components obtained from Raman images. The HDPE matrix is differentiated from the fillers by a narrow Raman band located at $\sim 1296\text{ cm}^{-1}$ corresponding to CH_2 twisting modes in the crystalline phase [11, 12], while the fillers by the features absent in HDPE and characteristic for CNCs or MWCNTs. The presence of CNCs is verified by the Raman band located at $\sim 1097\text{ cm}^{-1}$, corresponding to the C–O ring stretching modes and the β -1,4 glycosidic linkage (C–O–C) stretching modes between the glucose rings of the cellulose chains. [13, 14] The first-order G-band located at $\sim 1595\text{ cm}^{-1}$ is used to confirm the presence of carbon nanotubes. This Raman band is assigned to zone centre phonons of E_{2g} symmetry involving the in-plane bond-stretching motion of pairs of C sp^2 atoms. [15, 16]

Figures 2 and 3 present Raman images of CNCs-HDPE and MWCNTs-HDPE composites. The color scale in the Raman images depicts the intensity of selected Raman bands, where a dark brown color indicates the absence or significantly low intensity of these Raman bands and a yellow color specifies their highest intensity. Raman images also reflect the features of the surface morphology for the specific components of the composite. The yellow areas in Figures 2A correspond to the aggregates of CNCs and are verified by the intensity of the Raman band located at $\sim 1097\text{ cm}^{-1}$. The shape of the CNCs aggregates corresponds to the shapes observed in the SEM images. The aggregates of freeze-dried CNCs form irregular shapes. The image shown in Figure 2B primarily indicates the presence of HDPE matrix, reflected by the intensity of a Raman band located at $\sim 1296\text{ cm}^{-1}$. This image is almost a negative of Figure 2A.

In contrast to the CNCs-HDPE composites, the MWCNTs filler efficiently mixes with the PE matrix. The bright yellow/brownish areas observed in Figure 3A represent regions where the intensity of the Raman band centred at $\sim 1595\text{ cm}^{-1}$ (the G band) is strong. MWCNTs are mixed uniformly in the PE matrix without formation of large agglomerates. Figure 3B is an image of the intensity of the Raman band located at $\sim 1296\text{ cm}^{-1}$ corresponding to CH_2 twisting modes in polyethylene. A Raman image

corresponding to the presence of HDPE shows some areas where its intensity is higher relative to the filler.

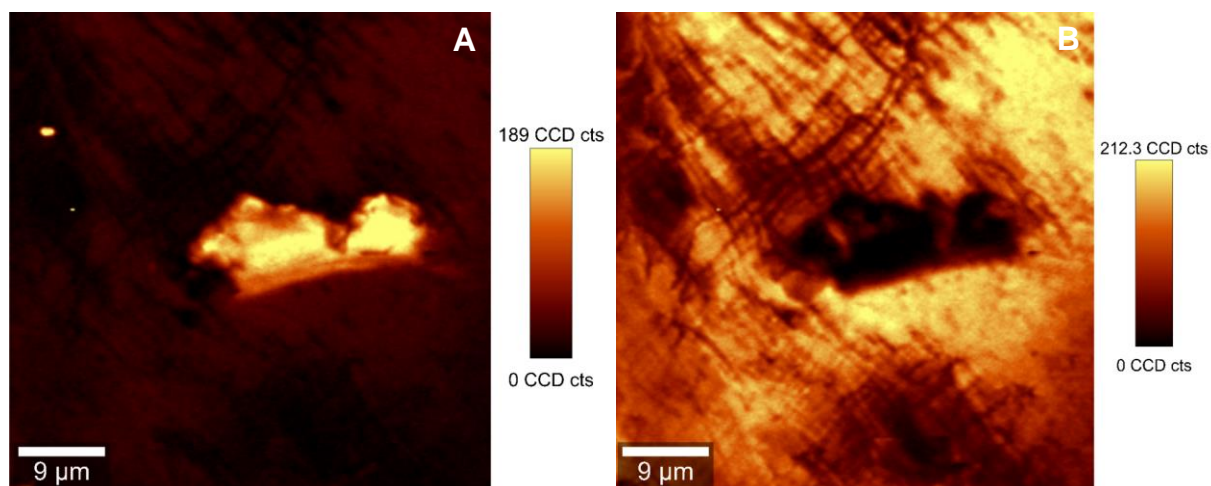


Figure 2. Typical Raman images of 1.25% CNCs-HDPE composite depicting the intensity of Raman band located at $\sim 1097\text{ cm}^{-1}$ (A) and $\sim 1296\text{ cm}^{-1}$ (B).

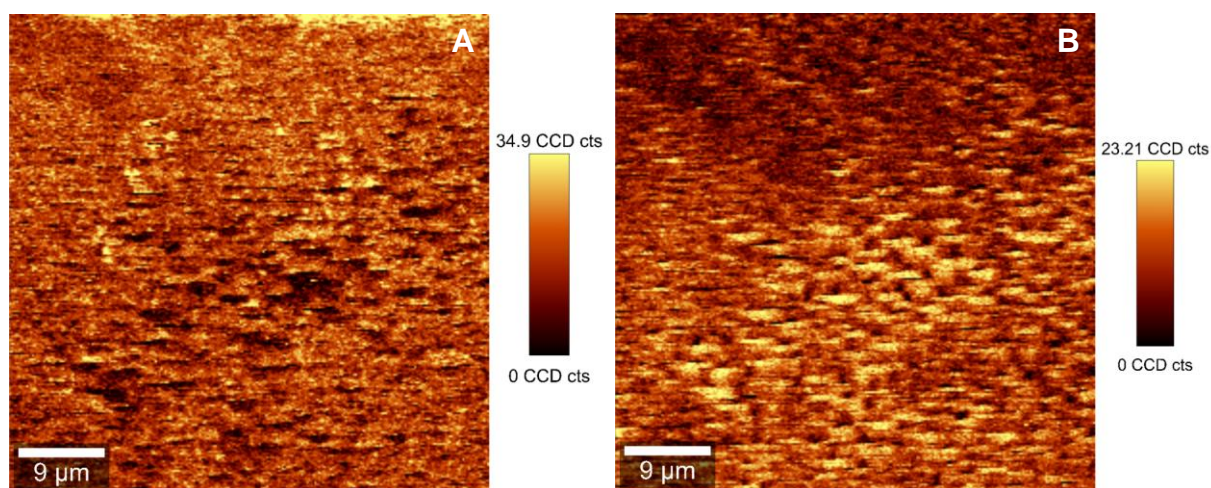


Figure 3. Typical Raman images of 1.25% MWCNTs-HDPE composite depicting the intensity of Raman band located at $\sim 1595\text{ cm}^{-1}$ (A) and $\sim 1296\text{ cm}^{-1}$ (B).

The conversion of Raman images to chemical images reveals regions corresponding to each of the composite components and the regions where mixing between fillers and matrix occurs (Figures 4A and 5A). The chemical image of the 1.25% CNCs-HDPE composite verifies once again the tendency of cellulose to aggregate within the HDPE matrix; both green and blue colors on Figure 4A. However, the chemical image reveals an additional feature corresponding to the cellulose aggregates. A large blue area of the aggregate is associated with mixing between CNCs and HDPE. A compound Raman spectrum corresponding to this region exhibits the bands characteristic of both CNCs and HDPE suggesting a good mixing of the components (Figure 4B - blue line). A Raman spectrum associated with the green area of the aggregate on the chemical map shows features characteristic of pure CNCs confirming the exclusive presence of the agglomerated filler in these areas (Figure 4B - green line).

The majority of the area on the chemical map of the composite is polyethylene matrix (Figure 4B - red line).

In contrast to CNCs-HDPE composites, a chemical map of 1.25% MWCNTs-HDPE illustrates an efficient mixing process between filler and polyethylene matrix (Figure 5A). It has to be noted however the given dimensions of the MWCNTs. The majority of the area in this chemical map corresponds to mixing between MWCNTs and HDPE. The compound Raman spectrum associated with this region shows features characteristic of both MWCNTs and HDPE (Figure 5B - green line). The presence of MWCNTs is indicated by the D and G bands, and HDPE by a narrow Raman band located at $\sim 1296\text{ cm}^{-1}$, and additionally by bands located at $\sim 1063\text{ cm}^{-1}$ and $\sim 1132\text{ cm}^{-1}$. [11, 12] Regions corresponding to pure HDPE is minimal in this chemical map (Figure 5B - red line spectrum).

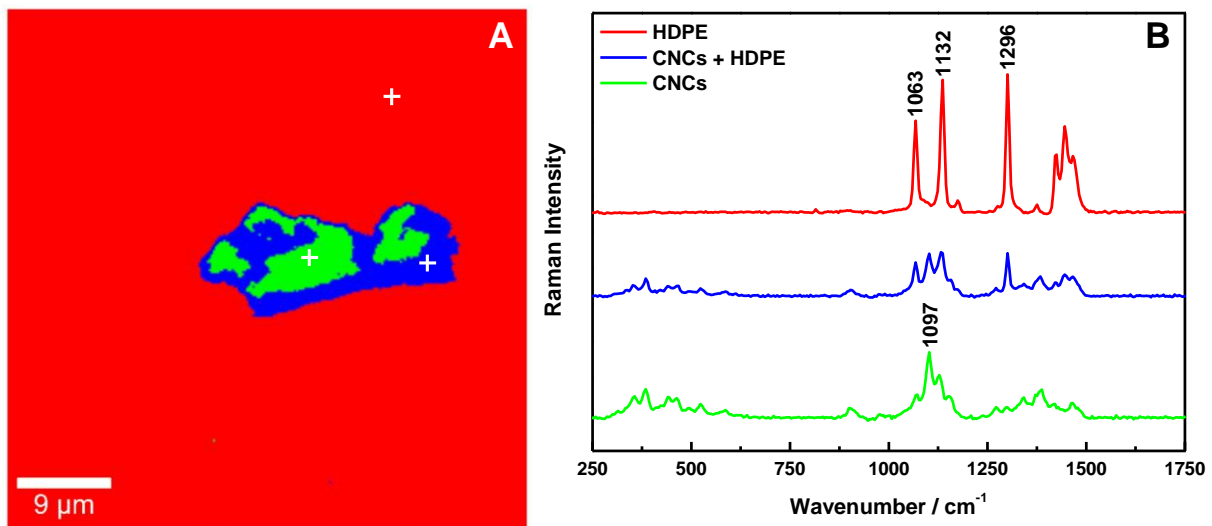


Figure 4. Typical chemical image of 1.25% CNCs-HDPE composite depicting the chemical composition of a mapped cross-section (A). Typical Raman spectra of composite components marked with the white crosses at the chemical image (B).

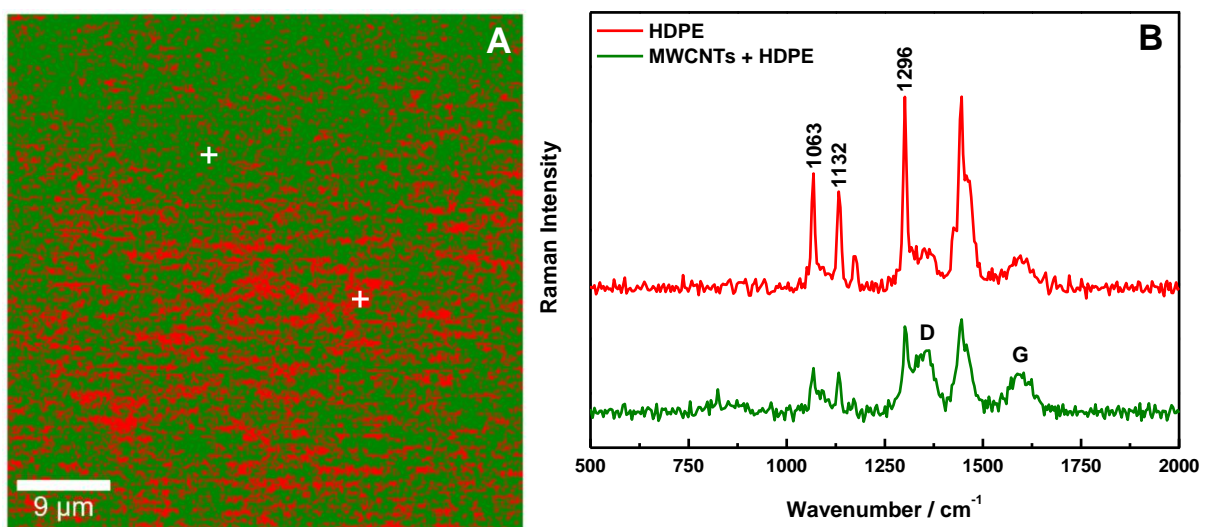


Figure 5. Typical chemical image of 1.25% MWCNTs-HDPE composite depicting the chemical composition of a mapped cross-section (A). Typical Raman spectra of composite components marked with the white crosses at the chemical image (B).

The degree of interaction between fillers and HDPE and the degree of agglomeration of the fillers are evaluated from the chemical images. Image J software was used to quantify the area in μm^2 related to the degree of mixing between the fillers and the matrix. The ratio of the fraction of the mixed areas (fillers and matrix) to the areas of pure matrix quantifies the effectiveness of the degree of mixing. This average ratio for 1.25% CNCs-HDPE composites (Blue area/Red area) is 0.06 ± 0.04 , while for 1.25% MWCNTs-HDPE composites (Green area/Red area) is 1.68 ± 0.52 . This clearly confirms the relatively higher degree of mixing of MWCNTs in polyethylene. The hydrophilic nature of CNCs induces the formation of hydrogen bonding between the nanoparticles increasing their tendency to agglomerate in nonpolar matrices.

4. Conclusions

The process of incorporation of fillers into thermoplastic matrices is highly important for their development as commodity materials. The formation of aggregates of fillers during the production stage is the main problem influencing the mechanical properties of the composites. Raman microscopy is a non-destructive and useful tool for chemical and spatial quantification of the mixing process of fillers in thermoplastics. The combination of the Raman images with chemical images delivers comprehensive spatial information regarding the agglomeration of fillers and above all quantifies the degree of mixing. Raman images reveal the formation of aggregates of CNCs in polyethylene and the absence of these aggregates for equivalent MWCNTs materials. Raman images provide a wider information about composite 'quality' supported by a detailed chemical quantification and a basic morphological feature of the material.

Acknowledgments

The authors would like to thank the EU FP7 funding programme for supporting the work under grant agreement no 604168 (www.newspec.eu). This publication reflects the views only of the author and the European Commission cannot be held responsible for any use which may be made of the information contained therein.

References

- [1] M. Pöllänen, M. Suvanto, T.T. Pakkanen. Cellulose reinforced high density polyethylene composites - Morphology, mechanical and thermal expansion properties. *Composites Science and Technology*, 76:21-28, 2013.
- [2] K. Ben Azouz, E.C. Ramires, W. Van den Fonteyne, N. El Kissi, A. Dufresne. Simple Method for the Melt Extrusion of a Cellulose Nanocrystal Reinforced Hydrophobic Polymer. *ACS Macro Letters*, 1:236-240, 2011.
- [3] J. Li, Z. Song, D. Li, S. Shang, Y. Guo. Cotton cellulose nanofiber-reinforced high density polyethylene composites prepared with two different pretreatment methods. *Industrial Crops and Products*, 59:318-328, 2014.
- [4] A.E. Lewandowska, M.A. Bañares. In situ TPR/TPO-Raman studies of dispersed and nano-scaled mixed V-Nb oxides on alumina. *Catalysis Today*, 118:323-331, 2006.
- [5] E. Mikolajaska, S.B. Rasmussen, A.E. Lewandowska, M.A. Bañares. Operando and in-situ Raman Studies of alumina-supported vanadium phosphate catalysts in propane ammoxidation reaction: Activity, selectivity and active phase formation. *Physical Chemistry Chemical Physics*, 14:2128-2136, 2012.

- [6] U.P. Agarwal, R. Sabo, R.S. Reiner, C.M. Clemons, A.W. Rudie. Spatially resolved characterization of cellulose nanocrystal-polypropylene composite by confocal Raman microscopy. *Applied Spectroscopy*, 66:750-756, 2012.
- [7] A.A. van Apeldoorn, H.-J. van Manen, J.M. Bezemer, J.D. de Bruijn, C.A. van Blitterswijk, C. Otto, Raman imaging of PLGA microsphere degradation inside macrophages. *Journal of the American Chemical Society*, 126:13226-13227, 2004.
- [8] E. Widjaja, M. Garland. Reverse engineering of multi-layer films. *Materials Today*, 14:114-117, 2011.
- [9] S. Huan, W. Lin, H. Sato, H. Yang, J. Jiang, Y. Ozaki, H. Wu, G. Shen, R. Yu. Direct characterization of phase behavior and compatibility in PET/HDPE polymer blends by confocal Raman mapping. *Journal of Raman Spectroscopy*, 38: 260-270, 2007.
- [10] R. Ou, Y. Xie, Q. Wang, S. Sui, M.P. Wolcott. Thermal, crystallization, and dynamic rheological behavior of wood particle/HDPE composites: Effect of removal of wood cell wall composition *Journal of Applied Polymer Science*, 131:40331(1-8), 2014.
- [11] H. Sato, M. Shimoyama, T. Kamiya, T. Amari, S. Šašić, T. Ninomiya, H.W. Siesler, Y. Ozaki. Raman spectra of high-density, low-density, and linear low-density polyethylene pellets and prediction of their physical properties by multivariate data analysis. *Journal of Applied Polymer Science*, 86:443-448, 2002.
- [12] S. S. Cherukupalli, A. A. Ogale. Online measurements of crystallinity using Raman spectroscopy during blown film extrusion of a linear low-density polyethylene. *Polymer Engineering & Science*, 44:1484-1490, 2004.
- [13] N. Gierlinger, M. Schwanninger. A. Reinecke, I. Burgert. Molecular changes during tensile deformation of single wood fibers followed by Raman microscopy. *Biomacromolecules*, 7:2077-2081, 2006.
- [14] R.H. Atalla, U.P. Agarwal. Raman microprobe evidence for lignin orientation in the cell walls of native woody tissue. *Science*, 227:636-638, 1985.
- [15] A.C. Ferrari, J. Robertson. Interpretation of Raman spectra of disordered and amorphous carbon. *Physical Review B*, 61:14095, 2000.
- [16] A.C. Ferrari, J. Robertson. Resonant Raman spectroscopy of disordered, amorphous, and diamondlike carbon. *Physical Review B*, 64:075414, 2001.